Communication

Journal of Nanoscience and Nanotechnology
Vol. 14, 2683–2686, 2014
www.aspbs.com/jnn

Carbon Nanofiber Interconnect RF Characteristics Improvement with Deposited Tungsten Contacts

Anshul A. Vyas[1,*], Francisco Madriz[1], Nobuhiko Kanzaki[1,2], Patrick Wilhite[1], Xuhui Sun[3], Toshishige Yamada[1,4], and Cary Y. Yang[1]

[1] TENT Laboratory, Department of Electrical Engineering, Santa Clara University, 500 El Camino Real, Santa Clara, CA 95053, USA
[2] Hitachi High-Technologies Corporation, Hitachinaka, Ibaraki, 317-8504, Japan
[3] FUNSOM, Soochow University, Suzhou, Jiangsu, 215123, China
[4] Electrical Engineering, University of California, Santa Cruz, Santa Cruz, CA 95064, USA

Carbon nanotubes (CNTs) and carbon nanofibers (CNFs) are potential materials for high-performance electronic devices and circuits due to their light weight and excellent electrical properties such as high current capacity and tolerance to electromigration. In addition, at high frequencies, these materials exhibit transport behavior which holds special promise for applications as on-chip interconnects. Contact resistance at CNF-metal interface is a major factor in limiting the electrical performance of CNF interconnects at all frequencies. In this paper, it is demonstrated that the contact resistance can be minimized and the high-frequency characteristics much enhanced by depositing tungsten on CNF-metal electrode contacts.

Keywords: Interconnect, Carbon Nanotubes, RF.

As the downward scaling of silicon integrated circuits (IC) continues, the shrinking of on-chip interconnects dimensions results in degradation in chip performance and reliability.[1] The resistivity of copper, currently the industry-standard interconnect material, increases exponentially with decreasing linewidth in the sub-30 nm regime due to grain-boundary scattering and surface scattering.[2,3] The scaling of interconnect dimensions has also resulted in an increase in the projected current density exceeding the maximum current-carrying capacity of Cu.[1] Thus, novel materials and structures in the nanoscale are needed to meet the demand of smaller and faster interconnects in next-generation ICs which operate at higher frequencies, in particular, transmission lines for broadband circuits. Frequency dependence in interconnect impedance and the presence of a reactive component can lead to undesirable resonance over the range of operating frequencies, which in turn significantly degrades circuit performance.

Materials in nanospace such as carbon nanotubes and graphene have been studied extensively for various applications in nanoelectronics,[1,4] due to their excellent electrical and thermal properties. Similar nanomaterials and nanostructures have also been investigated for other applications in nanospace.[5,6] In general, control in nanofabrication of these materials and device structures is key to successful functionalization and in achieving the optimal properties for the desired applications.[7,8] In particular, carbon nanotubes (CNTs) and carbon nanofibers (CNFs) are materials under investigation and exhibit promising properties for use as interconnects in the nanoscale.[9–15] They have been shown to possess much higher current capacity than Cu and are more tolerant to electromigration,[11,15] as well as other superior physical properties.[16–20] However, high resistance at the CNF-metal contact due to interface imperfections remains a major challenge.[11,15,16,20–24] Moreover, contact resistance tends to dominate the total resistance of the test device.[21,22] Previously, Madriz et al. developed a technique to characterize CNF interconnects by constructing a lumped-parameter circuit model based on S-parameter measurements.[25] Their findings led to the conclusion that it would be possible to model CNF as a constant resistor up to 50 GHz if the contact resistance is negligible. Preliminary experiments using Pt as a contact material revealed behavior of CNF approaching that of a frequency-independent resistor up to

*Author to whom correspondence should be addressed.

50 GHz. Saito et al. demonstrated that the contact resistance was substantially reduced by depositing tungsten (W) at the CNF-metal contacts.[26] However, those devices were characterized at dc only.

In this paper, improved electrical characteristics of CNFs with W contacts are reported for dc and frequencies up to 50 GHz. The resulting total dc resistance is drastically reduced and the linearity of the I–V characteristic is much improved. Further, we have characterized and modeled the frequency-dependent behavior of CNF test devices.[25,27–29] The results show definitively that using W-deposited electrode contacts, the CNF test device becomes a virtually frequency-independent resistor up to 50 GHz.

The test structure used for this experiment was the same as that used by Madriz et al. for their experiments on two-port device characterization.[25] The layout and design considerations for the test structure were described in detail elsewhere.[25,27] A three-dimensional schematic of the test structure layout is shown in Figure 1. In particular, the thickness of the SiO_2 layer should be made as large as possible to minimize pad-to-ground coupling. However, increasing the SiO_2 thickness enhances the capacitive coupling between the signal pads. Thus a trade-off exists.[25,27] Based on field-solver simulations and on measurement results from fabricated test structures, the thickness of the oxide between the ground plane and signal pads is chosen to be 3 μm. The two-port transmission measurements are conducted for open test structures with 2 μm, 2.5 μm, and 3 μm oxide thicknesses. The test structure with 3 μm oxide thickness is selected as it exhibits no resonance up to 50 GHz, while striking a reasonable balance between the pad-to-ground and signal pad capacitive couplings. The test structures were fabricated and patterned using standard Si IC process technology.

To fabricate the test device, CNFs with diameters 100–250 nm were first grown using plasma-enhanced chemical vapor deposition (PECVD) on an oxide-covered Si wafer, with Ni as the catalyst. The CNFs were dispersed in isopropyl alcohol, and then subjected to ultrasound for further dispersion. The resulting solution was drop-casted onto a substrate with patterned test structures. Devices having a single CNF bridging two signal pads were identified with a scanning electron microscope (SEM) and selected for electrical measurements.[27–29]

Figure 2(a) shows a SEM image of a typical drop-casted CNF test device. After identifying such devices and performing initial current–voltage measurements, each device was first subjected to constant-current stressing, which improves the CNF/Au interface,[24,30] thus reducing the contact resistance. While current stressing is effective in reducing contact resistance of the drop-cast devices,[23] it does not ensure a stable electrode contact. Thus it is essential that a more reliable technique is developed to form a stable ohmic contact for CNF interconnects. Toward this end, W is deposited onto the CNF/Au electrode contacts using ion-beam-induced deposition (IBID) technique, as shown in Figure 2(b). For IBID, we use a focused ion beam system with $W(CO)_6$ as the W source.[26] The optimum deposition spot size and separation between electrode contacts are selected based on the criterion of minimum tungsten spread along the length of CNF to avoid potential shorting of the device.[26]

High-frequency measurements of S-parameters are performed on CNF test devices before and after W deposition using a vector network analyzer (VNA). An appropriate

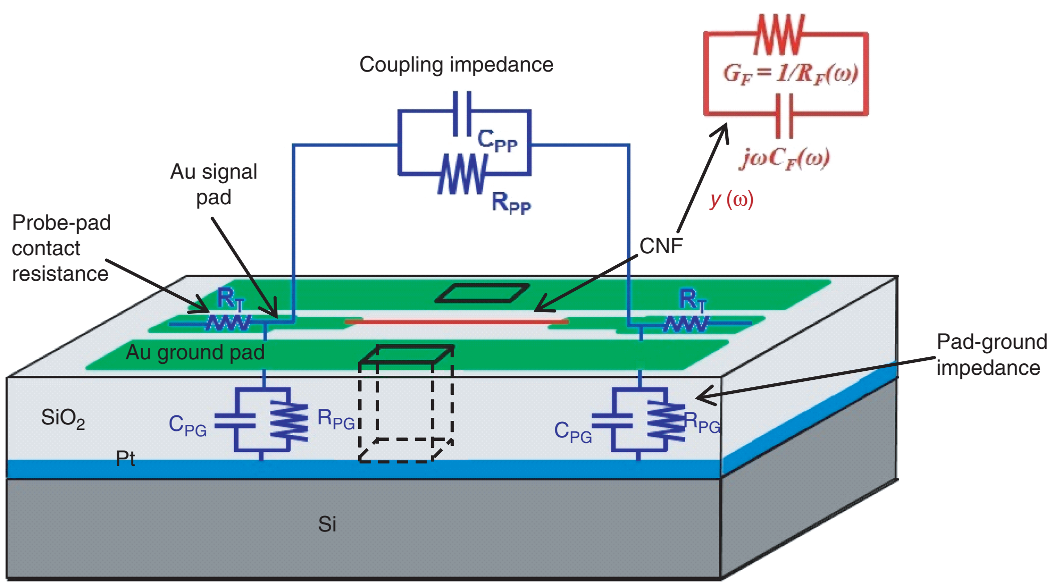

Figure 1. Schematic of the fabricated test structure together with its circuit model, where each model parameter is identified. $y(\omega)$ is the admittance of the circuit model for the CNF test device including its electrode contacts. An Au-filled trench connecting an Au ground pad to the Pt ground layer is indicated by broken lines.

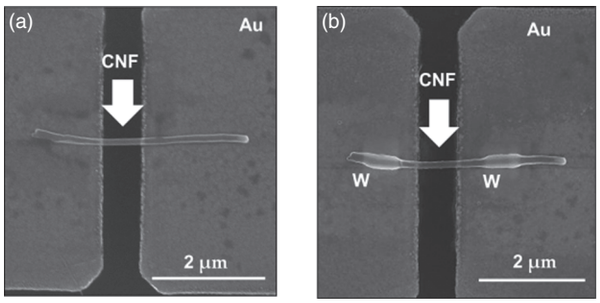

Figure 2. SEM images of (a) CNF test device after drop-cast and (b) CNF test device with W-deposited contacts.

Line-reflectance-Reflectance-Match (LRRM) calibration is carried out to remove the parasitics present in the VNA.[27] This technique is highly accurate and repeatable up to 50 GHz and beyond, with only ± 0.1 dB variations generally recommended for high-frequency measurements.[31] In addition, the parasitics inherent in the entire test structure are de-embedded to reveal the true characteristics of the CNF test devices. To implement such de-embedding, the open-structure admittance $Y_{21}^{\mathrm{OC}}(\omega)$ for the entire test configuration, whose model parameters are shown in Figure 1, is determined from the measured S-parameters. Subsequently, with the CNF test device in place, the S-parameters are measured again and the resulting admittance $Y_{21}^{\mathrm{CNF}}(\omega)$ is obtained. The CNF test devices admittance $y(\omega)$ is then given by[28]

$$y(\omega) = G_F(\omega) + j\omega C_F(\omega) = Y_{21}^{\mathrm{OC}}(\omega) - Y_{21}^{\mathrm{CNF}}(\omega) \quad (1)$$

Results for the extracted RC-circuit model parameters, R_F ($\equiv 1/G_F$) and C_F, for a typical test device are shown in Figure 3.

RF measurements and circuit modeling results for CNF interconnect test devices were first reported by Madriz et al.[27, 28] Those initial findings suggested that it would be possible to model CNF as a constant resistor up to 50 GHz provided that the contact impedance is negligible. Preliminary results using IBID-Pt as a contact material reduced the frequency variations of $R_F(\omega)$ and $C_F(\omega)$ to about 20% across the entire frequency range as compared to over 75% for the annealed contacts.[28] However, the current voltage (I–V) behavior of the Pt-contact devices was not ohmic, unlike those with deposited-W contacts.[26] Other metals such as Au, Pd, Nb, Ti, Cu, and graphitic carbon have been used as electrode contact materials to reduce contact resistance.[32–40] However, the results reported were obtained either at dc only or showed significant dependence of impedance on frequency. In particular, only one study was conducted up to 100 GHz showing strong dependence of impedance on frequency,[34] and the rest were at either dc or lower frequencies. Recently, graphitic carbon was studied as a contact material, which yielded low dc contact resistance.[40–42] In order to fully assess the potential for interconnect applications, high-frequency measurements and analysis are essential.

As shown in Figure 3, the total impedance of CNF devices after drop-cast is highly frequency-dependent. This frequency dependence is primarily due to the presence of contact impedance at the CNT/metal electrode interface. In order to enhance the potential of CNF for on-chip interconnect applications, such frequency dependence must be minimized. After IBID-W deposition, as shown in Figure 3, the frequency dependence of R_F is significantly reduced and C_F becomes vanishingly small. Thus the CNF test device including contacts can be modeled as a constant resistor. Saito et al.[26] demonstrated the use of W as a suitable electrode contact material to reduce the contact resistance and this finding has been confirmed by the results in Figure 3. Deposited W at the CNF/electrode contact yields an ohmic contact and contact impedance with a negligible reactive component, leaving the test device with only intrinsic CNF resistance and a small contact

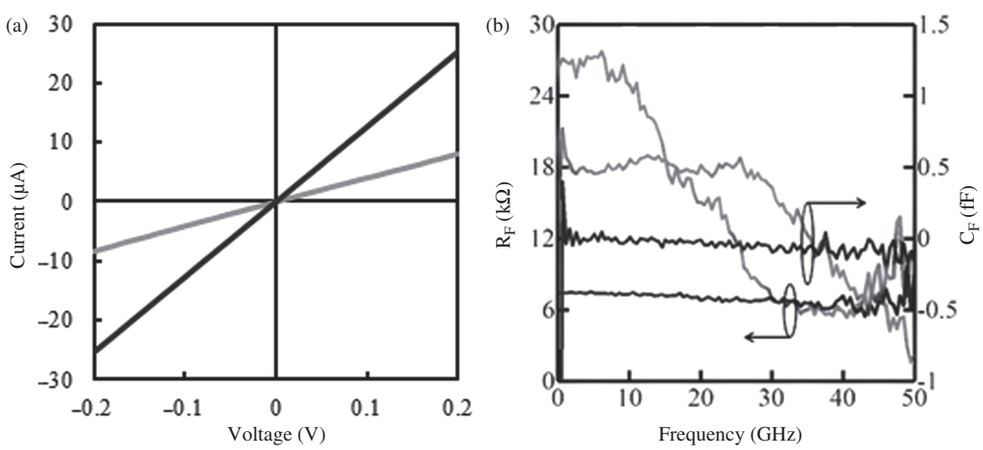

Figure 3. (a) I–V characteristics of a typical CNF test device before (grey) and after (black) W deposition using IBID. (b) Frequency dependence of circuit model parameters R_F and C_F for the same test device extracted from S-parameter measurements, before (grey) and after (black) formation of IBID-W contacts.

resistance. In addition, W deposition increases the effective contact area and improves the interface integrity at the electrode between the drop-casted CNF and the Au pad, thus drastically reducing unwanted tunneling transport across the interface, as supported by the linear I–V characteristics shown in Figure 3(a).[23, 24]

Our results show that the frequency dependence of CNF test device impedance is largely due to its contacts. Once the contact impedance is minimized, the CNF test device impedance becomes almost purely resistive, consisting of mostly CNF resistance. Such behavior is achieved with W-deposited electrode contacts for frequencies up to 50 GHz. The key in achieving such behavior lies in the reduction of contact impedance with W electrodes. W is compatible with Si IC fabrication process as it is used in interconnect vias. Thus, W electrode contacts for nanocarbons can lead to better assessment of their potential as next-generation on-chip interconnect materials. Further study is needed to determine if W compounds such as oxide and carbide are present at or near the electrode contact interface and their effects on the electrical properties of the CNF test device.

References and Notes

1. International Technology Roadmap For Semiconductors, 2011 edition with 2012 updates, http://www.itrs.net/Links/2012ITRS/Home2012.htm.
2. D. S. Gardner, J. D. Meindl, and K. C. Saraswat, *IEEE. Trans. Electron Devices* 34, 633 (**1987**).
3. H. Cho, K.-H. Koo, P. Kapur, and K. C. Saraswat, *Proc. IEEE IITC* (**2007**), p. 135.
4. K. Ariga, Q. Ji, J. P. Hill, Y. Bando, and M. Aono, *NPG Asia Mater.* 4, e17 (**2012**).
5. K. Ariga, A. Vinu, Y. Yamauchi, Q. Ji, and J. P. Hill, *Bull. Chem. Soc. Jpn*. 85, 1 (**2012**).
6. F. Ruffino and M. G. Grimaldi, *Nanosci. Nanotechnol. Lett.* 4, 309 (**2012**).
7. Q. Zhang, H. Xu, and W. Yan, *Nanosci. Nanotechnol. Lett.* 4, 505 (**2012**).
8. K. Ariga, T. Mori, and J. P. Hill, *Adv. Mater*. 24, 158 (**2012**).
9. M. S. Dresselhaus, G. Dresselhaus, and P. C. Eklund, Science of Fullerenes and Carbon Nanotubes, edited by M. S. Dresselhaus, Academic Press, San Diego (**1996**), p. 870.
10. C. Dekker, *Physics Today* 52, 22 (**1999**).
11. Y. Y. Wei and G. Eres, *Appl. Phys. Lett.* 76, 3759 (**2000**).
12. Kreupl, A. P. Graham, G. S. Duesberg, W. Steinhogl, M. Liebau, E. Unger, and W. Honlein, *Microelec. Eng.* 64, 399 (**2002**).
13. L. Zhang, D. Austin, V. I. Merkulov, A. V. Meleshko, K. L. Klein, M. A. Guillorn, D. H. Lowndes, and M. L. Simpson, *Appl. Phys. Lett.* 84, 3972 (**2004**).
14. M. Nihei, A. Kawabata, D. Kondo, M. Horibe, S. Sato, and Y. Awano, *Jpn. J. Appl. Phys. Part* 1 44, 1626 (**2005**).
15. Q. Ngo, T. Yamada, M. Suzuki, Y. Ominami, A. M. Cassell, J. Li, M. Meyyappan, and C. Y. Yang, *IEEE Trans. Nanotech.* 6, 311 (**2007**).
16. Y. Ominami, Q. Ngo, A. J. Austin, H. Yoong, C. Y. Yang, A. M. Cassell, B. A. Cruden, J. Li, and M. Meyyappan, *Appl. Phys. Lett.* 87, 233105 (**2005**).
17. M. Suzuki, T. Yamada, and C. Y. Yang, *Appl. Phys. Lett.* 90, 083111 (**2007**).
18. T. Yamada, F. R. Madriz, and C. Y. Yang, *IEEE Trans. Elec. Dev.* 56, 1834 (**2009**).
19. T. Yamada, H. Yabutani, T. Saito, and C. Y. Yang, *Nanotechnology* 21, 265707 (**2010**).
20. T. Yamada, T. Saito, D. Fabris, and C. Y. Yang, *IEEE Elec. Dev. Lett.* 30, 469 (**2009**).
21. W. Wu, S. Krishnan, T. Yamada, X. Sun, P. Wilhite, R. Wu, K. Li, and C. Y. Yang, *Appl. Phys. Lett.* 94, 163113 (**2009**).
22. K. Li, R. Wu, P. Wilhite, V. Khera, S. Krishnan, X. Sun, and C. Y. Yang, *Appl. Phys. Lett.* 97, 253109 (**2010**).
23. T. Yamada, T. Saito, M. Suzuki, P. Wilhite, X. Sun, N. Akhavantafti, D. Fabris, and C. Y. Yang, *J. Appl. Phys.* 107, 044304 (**2010**).
24. T. Yamada, *Appl. Phys. Lett.* 78, 1739 (**2001**).
25. F. R. Madriz, J. R. Jameson, S. Krishnan, X. Sun, and C. Y. Yang, *Proc. ICMTS* (**2009**), p. 36.
26. T. Saito, T. Yamada, D. Fabris, H. Kitsuki, P. Wilhite, M. Suzuki, and C. Y. Yang, *Appl. Phys. Lett.* 93, 102108 (**2008**).
27. F. R. Madriz, J. R. Jameson, S. Krishnan, K. Gleason, X. Sun, and C. Y. Yang, *Proc. IEEE IITC* (**2008**), p. 138.
28. F. R. Madriz, J. R. Jameson, S. Krishnan, X. Sun, and C. Y. Yang, *IEEE Trans. Elec. Dev.* 56, 1557 (**2009**).
29. F. R. Madriz, T. Yamada, X. Sun, J. G. Nickel, and C. Y. Yang, *IEEE Elec. Dev. Lett.* 31, 263 (**2010**).
30. H. Kitsuki, T. Yamada, D. Fabris, J. R. Jameson, P. Wilhite, M. Suzuki, and C. Y. Yang, *Appl. Phys. Lett.* 92, 173110 (**2008**).
31. A. J. Lord, *Proc. 29th Eur. Microw. Conf*., Munich, Germany (**1999**), Vol. 3, p. 28.
32. G. F. Close and H. S. P. Wong, *IEEE Trans. Nanotech.* 7, 596 (**2008**).
33. S. C. Jun, J. H. Choi, S. N. Cha, C. W. Baik, S. Lee, H. J. Kim, J. Hone, and J. M. Kim, *Nanotech*. 18, 255701 (**2007**).
34. S. C. Jun, X. M. H. Huang, S. Moon, H. J. Kim, J. Hone, Y. W. Jin, and J. M. Kim, *New J. Phys.* 9, 265 (**2007**).
35. J. J. Plombon, K. P. O'Brien, F. Gstrien, and V. M. Dubin, *Appl. Phys. Lett.* 90, 063106 (**2007**).
36. M. Zhang, X. Huo, P. C. H. Chan, Q. Liang, and Z. K. Tang, *IEEE Elec. Dev. Lett.* 217, 668 (**2006**).
37. L. Nougaret, G. Dambrine, S. Lepilliet, H. Happy, N. Chimot, V. Derycke, and J.-P. Bourgoin, *Appl. Phys. Lett.* 96, 042109 (**2010**).
38. A. A. Pesetski, J. E. Baumgardner, E. Folk, J. X. Prybysz, J. D. Adam, and H. Zhang, *Appl. Phys. Lett.* 88, 113103 (**2006**).
39. P. Rice, T. M. Wallis, S. E. Russek, and P. Kabos, *Nano Lett.* 7, 1086 (**2007**).
40. L.-G. Rojas, S. Bhatacharyya, E. Mendoza, D. C. Cox, J. M. Rosolen, and S. R. P. Silva, *Nano Lett.* 7, 2672 (**2007**).
41. Y. Chai, A. Hazeghi, K. Takei, H-Y. Chen, P. C. H. Chan, A. Javey, and H.-S. P. Wong, *IEEE Trans. Elec. Dev.* 59, 12 (**2012**).
42. S. Kim, D. D. Kulkarni, K. Rykaczewski, M. Henry, V. V. Tsukruk, and A. G. Fedorov, *IEEE Trans. Nanotech.* 11, 1223 (**2012**).

Received: 11 February 2013. Accepted: 23 March 2013.